The EMBO Journal (2010) 29, 3819–3825 | © 2010 European Molecular Biology Organization | Some Rights Reserved 0261-4189/10
www.embojournal.org

THE EMBO JOURNAL

EMBO open

Visualizing the transfer-messenger RNA as the ribosome resumes translation

Jie Fu[1], Yaser Hashem[2], Iwona Wower[3], Jianlin Lei[1,6], Hstau Y Liao[1], Christian Zwieb[4], Jacek Wower[3] and Joachim Frank[1,2,5]

[1]Department of Biochemistry and Molecular Biophysics, Columbia University, New York, NY, USA, [2]Department of Biochemistry and Molecular Biophysics, Howard Hughes Medical Institute, Columbia University, New York, NY, USA, [3]Department of Animal Sciences, Auburn University, Auburn, AL, USA, [4]Department of Molecular Biology, University of Texas Health Science Center at Tyler, Tyler, TX, USA and [5]Department of Biological Sciences, Columbia University, New York, NY, USA

Bacterial ribosomes stalled by truncated mRNAs are rescued by transfer-messenger RNA (tmRNA), a dual-function molecule that contains a tRNA-like domain (TLD) and an internal open reading frame (ORF). Occupying the empty A site with its TLD, the tmRNA enters the ribosome with the help of elongation factor Tu and a protein factor called small protein B (SmpB), and switches the translation to its own ORF. In this study, using cryo-electron microscopy, we obtained the first structure of an *in vivo*-formed complex containing ribosome and the tmRNA at the point where the TLD is accommodated into the ribosomal P site. We show that tmRNA maintains a stable 'arc and fork' structure on the ribosome when its TLD moves to the ribosomal P site and translation resumes on its ORF. Based on the density map, we built an atomic model, which suggests that SmpB interacts with the five nucleotides immediately upstream of the resume codon, thereby determining the correct selection of the reading frame on the ORF of tmRNA.

The EMBO Journal (2010) **29,** 3819–3825. doi:10.1038/emboj.2010.255; Published online 12 October 2010
Subject Categories: proteins; structural biology
Keywords: tmRNA; *trans*-translation; SmpB

Introduction

Translation of an mRNA that lacks a stop codon stalls the ribosome at the end of the message, and produces a defective polypeptide that may be toxic to the cell. In bacterial cells, this situation is resolved by a process called *trans*-translation (Tu *et al*, 1995; Keiler *et al*, 1996a). The key player in *trans*-translation is a highly structured molecule called the transfer-messenger RNA (tmRNA), which consists of a tRNA-like domain (TLD) that mimics a tRNA structurally and functionally (Gutmann *et al*, 2003; Bessho *et al*, 2007), an open reading frame (ORF) that encodes a degradation signal, and several pseudoknots and helices. Elongation factor Tu (EF-Tu) and an 18.3-kDa protein called small protein B (SmpB) also have important functions in *trans*-translation. Forming a complex with EF-Tu, GTP and SmpB, tmRNA occupies the empty A site with its TLD (Rudinger-Thirion *et al*, 1999; Valle *et al*, 2003). Acting like a tRNA, the TLD accepts the polypeptide from the P-site tRNA and is translocated to the P site, whereas the deacylated P-site tRNA moves to the E site. The ORF of the tmRNA is then placed into the ribosome, replacing the defective mRNA molecule (Williams *et al*, 1999; Ivanova *et al*, 2005). Translation resumes on the ORF until the ribosome reaches an internal stop codon on the ORF. Subsequently, the nascent polypeptide chain, which is now tagged by the signal encoded in the ORF, is released and targeted for degradation (Keiler *et al*, 1996b).

The initial stages of *trans*-translation, up to the point when TLD is accommodated to the ribosomal A site, have been visualized by cryo-EM. Structures of the tmRNA–ribosome complex solved to date include those of the pre-accommodation complex (Valle *et al*, 2003; Kaur *et al*, 2006), which reflects the state right before the accommodation of the TLD into the ribosomal A site, and the accommodation complex (Kaur *et al*, 2006; Weis *et al*, 2010), which reflects the state right after the accommodation of TLD in the A site. In the structures of the pre-accommodation complexes, the tmRNA pseudoknots form a solid arc around the head of the 30S subunit. Its TLD, positioned like an A/T-state tRNA, interacts with EF-Tu in a way similar to a canonical tRNA (Valle *et al*, 2003; Kaur *et al*, 2006). Thus, the cryo-EM structures confirmed the notion that the TLD is a structural and functional mimic of tRNA, and suggested that the pseudoknots most likely have a function in maintaining the complex topology of the tmRNA. In contrast to the solid structure of the pre-accommodation complex, the accommodation complex (Kaur *et al*, 2006; Weis *et al*, 2010) only showed fragmented density attributable to the tmRNA, suggesting structural variability resulting from flexibility of the complex and/or low occupancy of the tmRNA on the ribosome.

Two of the most intriguing questions are how the ribosome selects the correct reading frame on the ribosome and how tmRNA passes through the ribosome. Previous studies suggest that several nucleotides immediately upstream of the resume condon are important for establishing the

Corresponding author. Department of Biology, Biochemistry and Molecular Biophysics, Howard Hughes Medical Institute at Columbia University, 650 W. 168th Street, P&S Black Building 2-221, New York, NY 10032, USA. Tel.: +1 212 305 9510; Fax: +1 212 305 9500; E-mail: jf2192@columbia.edu
[6]Present address: School of Life Sciences, Tsinghua University, Beijing 100084, China

Received: 13 July 2010; accepted: 22 September 2010; published online: 12 October 2010

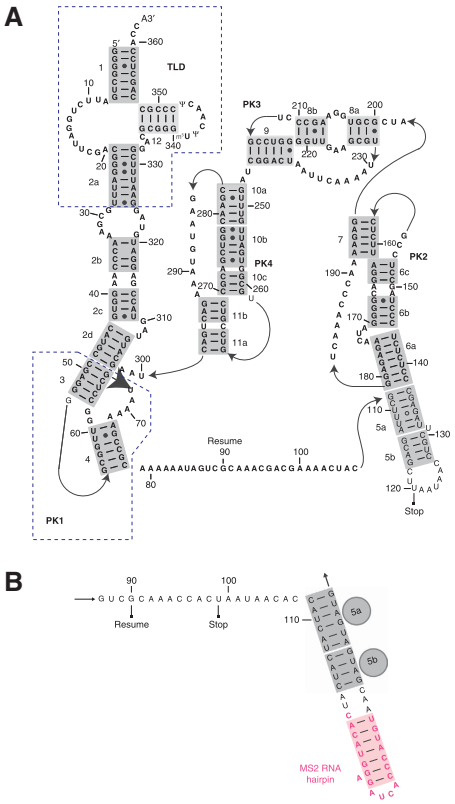

Figure 1 Secondary structure of the tmRNA. (**A**) Secondary structure of wild-type *E. coli* tmRNA. (**B**) Mutations and modifications made to the open reading frame (ORF) of the tmRNA to reduce sample heterogeneity. MS2 hairpin insertion is shown in magenta.

correct reading frame (Williams *et al*, 1999; Lee *et al*, 2001; Miller *et al*, 2008). The interaction between SmpB and tmRNA also appears to have a function in this process (Konno *et al*, 2007; Metzinger *et al*, 2008; Watts *et al*, 2008, 2009). Biochemical and genetics methods have been used to investigate the manner in which the tmRNA passes through the ribosome, in the later stages of *trans*-translation (Ivanov *et al*, 2002; Wower *et al*, 2005; Ivanova *et al*, 2007; Bugaeva *et al*, 2008). Because of the complex topology of tmRNA, some researchers suggested that the tmRNA has to unfold extensively in order to pass through. However, without understanding of the structural aspects of these later processes, the answers to these questions remain elusive.

Here, we set out to study the structure of a functional tmRNA–ribosome complex in the later stages of *trans*-translation. We purified the complex directly from the cell in order to study the native states in the process of *trans*-translation. By introducing strategic mutations for stabilization of the tmRNA–ribosome complex and using a novel classification method (Scheres *et al*, 2007) for sorting out the coexisting conformations, we were able to obtain the structure of the complex at the point where the TLD has moved to the P site and translation is resumed on the ORF of tmRNA. Our results show that, similar as in the pre-accommodation complex, the tmRNA forms a stable, albeit differently positioned 'arc and fork' structure on the ribosome at this point. Our atomic model based on the cryo-EM density map defines the contacts of the tmRNA with the ribosome, and sheds light on the process by which the ribosome selects the correct reading frame on the tmRNA.

Results

To study the native states in the *trans*-translation processes, we formed the tmRNA–ribosome complex *in vivo*. We took several measures to address the anticipated problem of heterogeneity in the specimen. To improve the occupancy of the tmRNA on the ribosome, we inserted an MS2-binding hairpin (hp) into the helix 5 of tmRNA (Figure 1), so that only those ribosome complexes that were bound with tmRNA were purified. To reduce the structural heterogeneity, we mutated the 4th and 5th sense codons of the MS2-tmRNA to UAA stop codons, expecting that the complex formed by this tmRNA mutant and the ribosome would be less flexible because translation would be stopped at an earlier stage, thus reducing the number of different possible conformations of the complex.

The tmRNA–ribosome complexes are in the resume state

Initial reconstruction of the complex showed a 70S ribosome structure with an extra density around the beak of the 30S subunit (Supplementary Figure S1A). Fragmented densities, which cannot be attributed to the 70S ribosome, show up at reduced threshold, suggesting the presence of structural heterogeneity (data not shown). Thus, we applied the maximum-likelihood (ML) classification method (Scheres *et al*, 2007) to sort the data set into multiple classes (Supplementary Figure S1). Separate reconstructions of the classes generated multiple distinct density maps with resolutions in the range of 13–18 Å (Supplementary Figures S1 and S2; Supplementary Table S1). For further structural analysis,

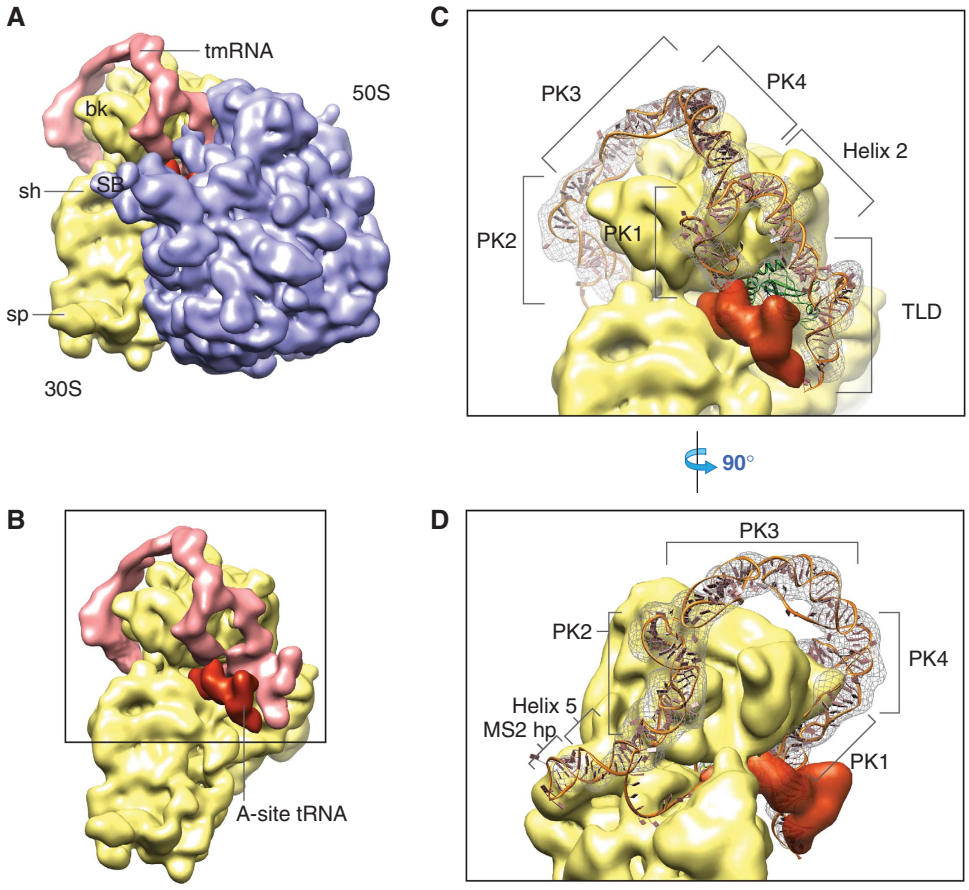

Figure 2 Cryo-EM density map of the tmRNA–ribosome complexes in the resume state. (**A**) 70S ribosome in complex with tmRNA. 50S subunit is coloured in blue, 30S subunit is in yellow, tmRNA is in pink and A-site tRNA is in red. (**B**) 30S subunit and ligands isolated from the cryo-EM map, viewed from the inter-subunit side. (**C**) Atomic models of tmRNA and SmpB superimposed with the cryo-EM density, zoomed in on the region outlined in (**B**). The backbone of the tmRNA is coloured in orange, bases are in pink and SmpB is in green. (**D**) Same content as in (**C**), viewed from the 30S solvent side. Landmarks used in all the figures: bk, beak; sh, shoulder; SB, base of the L7/L12 stalk; CP, central protuberance; PK1–PK4, pseudoknots; TLD, tRNA-like domain; MS2 hp, MS2 protein-binding hairpin.

we excluded those maps that contain fragmented densities for tmRNA (Structures 1–5 in Supplementary Figure S1). The remaining map is reconstructed from 20 873 projection images, and has a resolution of 13.6 Å. The crystal structure of the *Escherichia coli* 70S ribosome (Schuwirth *et al*, 2005) was fit into the cryo-EM density map using real-space refinement, a procedure which locally optimizes the cross-correlation between pieces of the atomic model and the density map (Gao *et al*, 2003). After obtaining an atomic model for this cryo-EM map, we were able to accurately subtract the densities attributed to the ribosome from the cryo-EM map. Part of the remaining density mass is situated at the A site and has the shape and size of a tRNA even when the map is displayed at high threshold, suggesting solid binding of a tRNA at the A site (Figure 2B).

The remaining density, after excluding the A-site tRNA, was compared with the tmRNA density isolated from the pre-accommodation complex (Kaur *et al*, 2006) (Figure 3). The similarity of the two maps can be readily seen: both maps contain the arc structure, which is connected to a fork structure that extends to the inter-subunit space of the ribosome. In the density of the pre-accommodation complex (Kaur *et al*, 2006), the fork structure extends to the TLD in the A/T position, whereas in the density we have now obtained, the fork structure extends to a ligand at the ribosomal P site. Based on the similarity of this density with the previous cryo-EM maps, and the connectivity of the TLD with the rest of the tmRNA, we conclude that this density must be attributed to the tmRNA, and specifically, the P-site ligand mass must be attributed to the TLD. In addition, when displayed at lower threshold, a thin strand of density, which is attributed to a highly stabilized single-stranded RNA, can be seen extending from the anticodon end of the A-site tRNA into the mRNA entry channel. This indicates the incorporation of the ORF into the ribosome (Supplementary Figure S3). Thus, the complex is apparently in the state where TLD has been translocated to the P site and translation has resumed on the first ORF codon. We confirmed this conclusion with northern blot analysis (see Materials and methods): the tRNAs in the tmRNA–ribosome complex is predominantly Ala-tRNA (Supplementary Figure S4), thus the first codon of the ORF on the mRNA-like domain must be at the A site. We term this state the *resume state* and the corresponding complex the *resume complex*.

Atomic model built based on the cryo-EM density allows for detailed interpretation

To interpret the density of the tmRNA, we built an atomic model of the tmRNA using homology and *ab initio* modelling techniques, starting from 2D structural alignment and X-ray

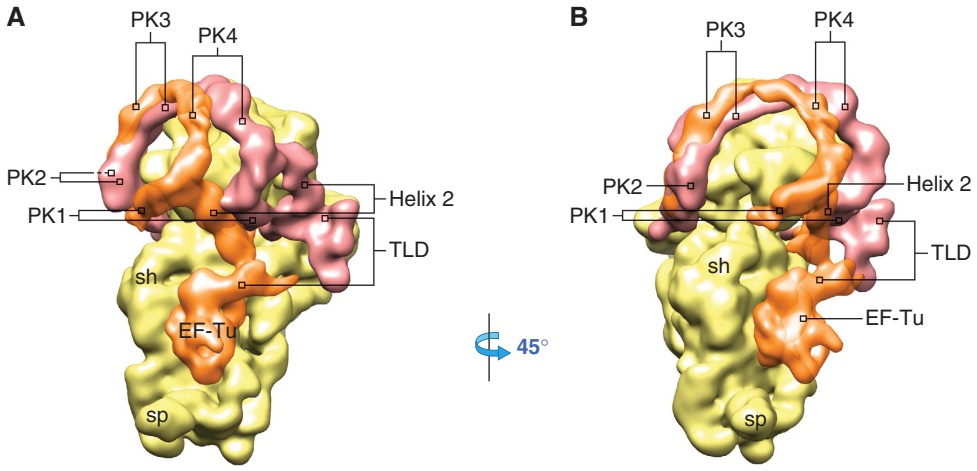

Figure 3 Superimposition of tmRNAs in the pre-accommodation state (orange) and in the resume state (pink). The 30S subunit, shown in yellow, is from the *resume complex*. (**A**) Superimposed structures viewed from the 30S inter-subunit side. (**B**) Same structures viewed from the inter-subunit side.

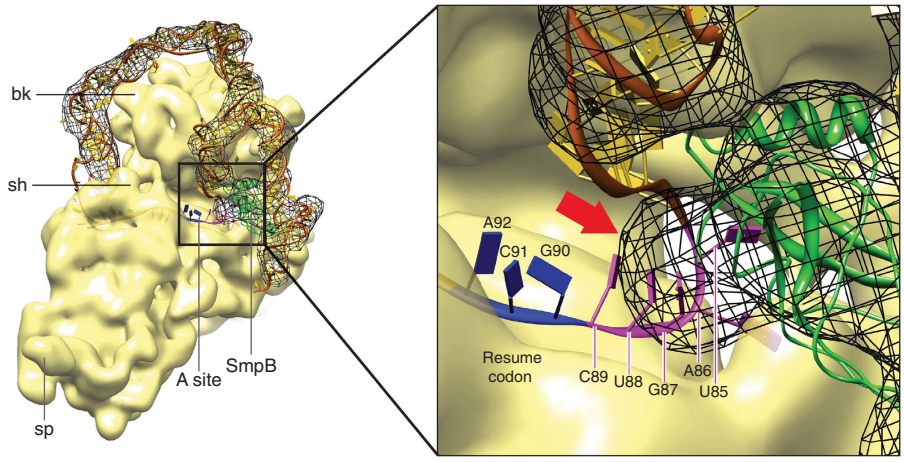

Figure 4 Interaction of the SmpB with the five nucleotides immediately upstream of the resume codon. (Left) Cryo-EM density of the 30S subunit and tmRNA, superimposed with the atomic models, viewed from the inter-subunit space. (Right) Zoomed-in view of the region outlined in the left panel. The crystal structure of the *T. thermophilus* SmpB (in green) is superimposed with the density. The backbone of the tmRNA model is coloured in orange and bases in yellow, except for the resume codon (coloured in blue) and the five nucleotides upstream of it (in magenta). Red arrow indicates the part of the density that contacts the five upstream nucleotides.

structures of homologous domains deposited in the PDB (see Experimental Procedure and Supplementary Figure S5). Based on biochemical data and structural evidence (Gutmann *et al*, 2003; Valle *et al*, 2003), we were able to determine the locations of these components unambiguously and place the atomic model into the density map. Despite the good fit of our model in the density map, several runs of molecular dynamic flexible fitting, which uses the density map as a force potential to drive models into the map during simulation, were additionally performed (Trabuco *et al*, 2008). The resulting conformation displays a better cross-correlation coefficient (CCC) and root mean square deviation (RMSD) with the density map than the initial model (Supplementary Figure S6).

tmRNA undergoes large conformational changes from the pre-accommodation to the resume state

With all the components of the tmRNA assigned, we can analyse the large conformational rearrangement that occurs during the transition from the pre-accommodation state to the *resume state*. Apparently, although one end of the arc, pseudoknot PK2, remains bound at similar positions on the 30S subunit, the other end, pseudoknot PK1, moves towards the inter-subunit space and down towards the codon recognition centre. Simultaneously, helix 2 and TLD moves all the way into the inter-subunit space (Figure 3). Evidently, the large conformational change enabled both the translocation of the TLD to the P site and the insertion of the ORF, which is downstream of pseudoknot PK1 but upstream of pseudoknot PK2.

Interaction of SmpB with the tmRNA contributes to the correct selection of the reading frame

As mentioned above, the TLD is located at the ribosomal P site. It is known that TLD and bound SmpB jointly mimic the structure of tRNA (Gutmann *et al*, 2003; Cheng *et al*, 2010). We observed that the P-site ligand has weaker density near the decoding centre. As protein results in weaker EM density than RNA, we conclude that in the *resume state* complex, SmpB mimics the anticodon arm of the normal P-site tRNA (Figure 4). We fitted the crystal structure of the *Thermus thermophilus* SmpB into our *E. coli* SmpB density. As shown in Figure 4, the density appears to be bigger than the crystal

structure. We can explain this discrepancy as due to the fact that *E. coli* SmpB has an extra segment of 26 amino acids on the C-terminal tail.

The SmpB appears to have an instrumental function in establishing the correct reading frame during *trans*-translation. At the 30S ribosomal P site, the SmpB density has direct contact with at least five nucleotides upstream of the resume codon, comprising the −1 triplet the U85 and the A86 nucleotides (Figure 4). As a result, the resume codon is precisely placed at the ribosomal A site.

Discussion

By reconstructing the structure of a tmRNA–ribosome complex formed *in vivo*, we obtained the first structures of the tmRNA–ribosome complex in the *resume state*, the state where translation is ready to resume on the ORF of the tmRNA. Our structure of the *resume complex* shows that tmRNA maintains a stable structure, at least up to this point.

Based on the cryo-EM density, we built an atomic model that allows for interpretation of the structure in great details. Generally, pseudoknots are known to be stable and robust structures. In the tmRNA model, successive pseudoknots are linked to each other by single-stranded regions and form an arc-like structure, giving the tmRNA the flexibility required for undergoing the observed large conformational changes from the pre-accommodated to the *resume state*, despite the structural robustness of the constitutive pseudoknots. The TLD displays clear structural resemblance with tRNA. It is connected to the arc of the pseudoknots by helix 2, which includes several mismatches and internal loops.

The fact that we observe only the *resume complex* suggests that the translation process is slowed down in the resume state, and once the complex has passed through this state, translation will continue until the tmRNA–ribosome complex dissociates. Our atomic model suggests that the insertion of the MS2 hp may account for the slowing down of the process. The MS2 hp appears to stabilize helix 5, keeping it from unwinding. At least five of the ORF codons, including the stop condon, are contained in the structure of the helix 5 and its apical loop. Therefore, part of the helix 5 needs to be unpaired in order to be rendered completely accessible for translation by the resume-state ribosome.

How the correct reading frame is established, at the point where the ribosome switches from the stalled mRNA to the ORF of the tmRNA, has remained a crucial question in the study of *trans*-translation. As described in the Results section, our cryo-EM density and atomic model show that the SmpB interacts with the upstream region of the resume codon, thus presenting the resume codon at the A site. This is consistent with several previous studies, which showed that mutations on the five nucleotides immediately upstream of the resume codon cause frame shifting and *partial or complete* abolition of the tmRNA activity (Williams *et al*, 1999; Lee *et al*, 2001; Trimble *et al*, 2004; Lim and Garber, 2005; Konno *et al*, 2007; Miller *et al*, 2008). On the other hand, SmpB, which has been shown to bind with the upstream region of the resume codon (Konno *et al*, 2007; Metzinger *et al*, 2008), appears to contribute to the reading frame selection. One study showed that certain mutations on SmpB restore the function of the tmRNA with mutation on its resume codon upstream sequence (Watts *et al*, 2008, 2009).

Our atomic model, combined with the aforementioned genetic and biochemical studies, suggests that the reduction, abolition and frame shifting of the *trans*-translation activity is due to the incorrect presentation of the resume codon to the A site, subsequent to the alteration of the interaction between the SmpB and the resume codon upstream region. To investigate the details of the interaction between the SmpB and tmRNA, we modelled the extra C-terminal segment, which is present in the *E. coli* SmpB but not in the *T. thermophilus* SmpB, as a long helix (see Materials and methods), and fitted this helix into the cryo-EM density along with the crystal structure of the *T. thermophilus* SmpB. Our fitted model suggests that the −1 triplet, the U85 and A86 nucleotides may interact with residues 134–140 of the SmpB. It is also possible that other contacts may be established, through amino acids 18–24 of the SmpB and U85 and A86 nucleotides of the tmRNA (Supplementary Figure S7). Because of the limited resolution of our cryo-EM density, the exact nature of the interaction between the upstream region and the SmpB has not been addressed. However, because of the relative tolerance to modifications of the upstream sequence (Miller *et al*, 2008), the interaction could rely partly on contacts with the nucleotide's backbone. The length of the upstream sequence, according to our model, may also be a determinant for the optimal interaction with the SmpB, and consequently, for the presentation of the resume codon at the A site.

Another major question to be answered in the study of *trans*-translation is how tmRNA passes through the ribosome despite its complex topology. Our structures show that tmRNA has a great degree of structural flexibility: as mentioned above, in five of the six structures obtained by ML classification, the tmRNA densities are fragmented, whereas the density of the tRNA and the ribosome are solid. As all our complexes have TLD in the P site, the fragmentation seems to suggest that tmRNA starts to unfold after the TLD is translocated to the P site. On the other hand, our atomic model shows that the tmRNA is composed of stable structural elements that are difficult to unwind. In addition, the atomic model does not seem to be subjected to significant topological constraints, at least up to the point where tmRNA is translocated to the E site. More structural studies need to be done to further investigate this question.

Materials and methods

Preparation of MS2-tmRNA-4 mutant

MS2-tmRNA(H8), a variant of *E. coli* tmRNAH8 that can bind the coat protein from MS2 bacteriophage, was constructed by PCR-directed mutagenesis as described earlier (Wower *et al*, 2004). The resulting mutant is called MS2-tmRNA-4 (see also Figure 1B and Supplementary Materials and methods).

Protein tagging by MS2-tmRNA-4

E. coli strain IW363 was transformed with plasmid pETrpmA-At-3, which carries one copy of an *rpm*A gene encoding a truncated ribosomal protein L27, one copy of SmpB gene and one copy of modified *ssr*A gene encoding MS2-tmRNA-4 (Wower *et al*, 2004). Synthesis of truncated ribosomal protein L27 and following tagging activity was induced by addition of 1 mM IPTG to logarithmically growing cells and incubation was carried for 3 h. The expression of truncated protein L27 and its tagging were analysed by SDS–polyacrylamide electrophoresis as described in Wower *et al* (2004).

Purification of MS2-tmRNA-4:ribosome complexes

See Supplementary Materials and methods.

Identity of tRNA present in the affinity purified complexes

The identity of the tRNA was established by Northern hybridization with ^{32}P-labelled probes directed against *E. coli* $tRNA^{Ala}$, $tRNA^{Asn}$ or $tRNA^{His}$. All RNAs were synthesized *in vitro* using T7 RNA polymerase and purified by denaturing PAGE. See Supplementary Materials and Methods for synthesizing $tRNA^{Ala}$, $tRNA^{Asn}$ and $tRNA^{His}$. Total RNA was extracted from two A_{260} units of purified tmRNA-70S ribosome complexes using the RNAqueous-Micro kit (Ambion). In all, 1/20 of the extract was resolved on a 10% urea-polyacrylamide gel with 50 ng of purified tRNA transcripts. RNAs were blotted onto Zeta-Probe membrane in a semi-dry cell (Bio-Rad). Hybridizations were carried out in UlraHyb-Oligo (Ambion) solution with ^{32}P-labelled oligonucleotide probes: 5′-GAC CTC CTG CGT GC-3′ (for $tRNA^{Ala}$), 5′-GAC ATA CGG ATT AAC AG-3′ (for $tRNA^{Asn}$) and 5′-GGA ATC ACA ATC CAG G-3′ (for $tRNA^{His}$). Northern analyses were quantified using Typhoon PhosphoImager and ImageQuant 5.2 software. *E. coli* $tRNA^{Ala}$ was identified as the prominent species in the complexes. Only trace amounts of *E. coli* $tRNA^{His}$ were observed.

Electron microscopy and image processing

The tmRNA–ribosome specimen was diluted into a final concentration of 32 nM. A cryo-grid (carbon-coated Quantifoil 2/4 grid, Quantifoil Micro Tools GmbH, Jena, Germany) was prepared following standard cryo-procedures (Grassucci *et al*, 2007). Microscopy was performed under low-dose conditions on an FEI (FEI, Hillsboro, OR) Tecnai Polara instrument operating at 300 kV and a nominal magnification of $\times$ 59 000. Micrographs were recorded on a 4 $\times$ 4 k 16-bit TVIPS TemCam-F415 CCD camera, with a physical pixel size of 15 μm by using the automated data collection system AutoEMation (Lei and Frank, 2005). The effective magnification on the CCD was $\times$ 100 000 due to a post-magnification ratio of 1.7, thus making the pixel size 1.5 Å on the object scale. Micrographs were subsequently decimated to a 3 Å pixel size to boost the low-spatial frequency signal and reduce the processing time. Ribosome particles were windowed out from the micrographs using an automatic particle picking program (Rath and Frank, 2004). After manual verification, 90 894 particles were selected for single-particle classification and reconstruction, following standard SPIDER protocols for reference-based reconstruction (LeBarron *et al*, 2008; Shaikh *et al*, 2008). ML classification (Scheres *et al*, 2007) was performed using the XMIPP package (see Supplementary Materials and methods). The classification was done in a hierarchical manner as described in Supplementary Figure S1. The fitting of the atomic model was done in multiple steps using a combination of manual and real-space refinement fitting, as described in the text. The real-space refinement program used was RSREF (Chapman, 1995; Gao *et al*, 2003), and the initial atomic models were from the crystal structure of the *E. coli* ribosome (PDB codes: 2AVY and 2AW4 (Schuwirth *et al*, 2005)). The head of H38 was taken from PDB structure 1PNY (Vila-Sanjurjo *et al*, 2003).

Modelling of the tmRNA and SmpB

Both homology and *ab initio* modelling techniques were used to build the 3D atomic model of the tmRNA. The initial structural alignment was retrieved on the Rfam website (http://rfam.sanger.ac.uk/), then realigned in reference to the *E. coli* tmRNA sequence with the S2S tool (Jossinet and Westhof, 2005), against 228 tmRNA sequences (Supplementary Figure S5). The 3D atomic model was built with Assemble (Jossinet *et al*, 2010) and regular helices were generated directly from the sequence. Pseudoknots were also built with Assemble, based on existing structures of pseudoknots found by browsing the non-redundant database of X-ray structures. The TLD region was modelled by homology by applying the fold of the TLD crystal structure from *T. thermophilus* (Bessho *et al*, 2007). The crystal structure of the *T. thermophilus* SmpB (PDBID: 2CZJ) was fitted into our cryo-EM density map after verification of the good sequence homology between the *T. thermophilus* and *E. coli* SmpB. The remainder of the *E. coli* C-terminal tail is predicted to be a long helical segment by the SYMPRED consensus secondary structure prediction web service (http://www.ibi.vu.nl/programs/sympredwww/) with the PROF (Rost, unpublished data), SSPRO (Pollastri *et al*, 2002), YASPIN (Lin *et al*, 2005) and PSIPRED (McGuffin *et al*, 2000) methods. A 20 amino acids long α helix was modelled using PyMol (The PyMOL Molecular Graphics System, Version 1.2r3pre, Schrödinger, LLC) and fitted into the density to demonstrate the possibility of the interaction with the resume codon upstream region.

Molecular dynamics flexible fitting

The system was set up in VMD by adding a solvent box of ~4 00 000 TIP3P water molecules by using the SOLVATE module implemented in VMD, and neutralized by adding K ions. A 0.2 mol/l of K^+ ions has been added to the neutralized system. Ions were added using the ADDIONS module in VMD. CHARMM force field parameters were used (Combined CHARMM All-Hydrogen Topology File for CHARMM22 Proteins and CHARMM27 Lipids (MacKerell *et al*, 1998)), and the simulation was conducted using NAMD (Phillips *et al*, 2005). Trajectories of several nanoseconds were obtained for the cryo-EM density of the *resume state*. The final fitted structures were selected based on the RMSD and the CCC, after reaching a plateau within 400 ps of simulation time (Supplementary Figure S6).

All figures were rendered with UCSF Chimera (Pettersen *et al*, 2004).

Accession number

PDB IDs: the coordinates for the modelled and refined *E. coli* tmRNA has been deposited in the Protein Data Bank with accession numbers: 3IZ4. The cryo-EM maps have been deposited at the 3D-EM database, EMBL with accession numbers: EMD-5234.

Supplementary data

Supplementary data are available at *The EMBO Journal* Online (http://www.embojournal.org).

Acknowledgements

We thank Bob Grassucci for assistance with the microscopy, Lila Rubinstein and Melissa Thomas for assistance in the preparation of the illustrations, Fabrice Jossinet and Eric Westhof for their assistance in modelling the tmRNA molecule and Jiang Zhu for helpful discussions. This work was supported by HHMI and NIH R01 GM29169 (to JF), P01 GM064692 (to Robert M Glaeser) and R01 GM58267 (to JW).

Conflict of interest

The authors declare that they have no conflict of interest.

References

Bessho Y, Shibata R, Sekine S, Murayama K, Higashijima K, Hori-Takemoto C, Shirouzu M, Kuramitsu S, Yokoyama S (2007) Structural basis for functional mimicry of long-variable-arm tRNA by transfer-messenger RNA. *Proc Natl Acad Sci USA* **104:** 8293–8298

Bugaeva EY, Shpanchenko OV, Felden B, Isaksson LA, Dontsova OA (2008) One SmpB molecule accompanies tmRNA during its passage through the ribosomes. *FEBS Lett* **582:** 1532–1536

Chapman MS (1995) Restrained real-space macromolecular atomic refinement using a new resolution-dependent electron-density function. *Acta Crystallogr A* **51:** 69–80

Cheng K, Ivanova N, Scheres SHW, Pavlov MY, Carazo JM, Hebert H, Ehrenberg M, Lindahl M (2010) tmRNA·SmpB complex mimics native aminoacyl-tRNAs in the A site of stalled ribosomes. *J Struct Biol* **169:** 342–348

Gao H, Sengupta J, Valle M, Korostelev A, Eswar N, Stagg SM, Van Roey P, Agrawal RK, Harvey SC, Sali A, Chapman MS, Frank J (2003) Study of the structural dynamics of the E. coli 70S ribosome using real-space refinement. *Cell* **113:** 789–801

Grassucci RA, Taylor DJ, Frank J (2007) Preparation of macromolecular complexes for cryo-electron microscopy. *Nat Protoc* **2:** 3239–3246

Gutmann S, Haebel PW, Metzinger L, Sutter M, Felden B, Ban N (2003) Crystal structure of the transfer-RNA domain of transfer-messenger RNA in complex with SmpB. *Nature* **424:** 699–703

Ivanova N, Lindell M, Pavlov M, Holmberg Schiavone L, Wagner EG, Ehrenberg M (2007) Structure probing of tmRNA in distinct stages of trans-translation. *RNA* **13:** 713–722

Ivanova N, Pavlov MY, Ehrenberg M (2005) tmRNA-induced release of messenger RNA from stalled ribosomes. *J Mol Biol* **350:** 897–905

Ivanov PV, Zvereva MI, Shpanchenko OV, Dontsova OA, Bogdanov AA, Aglyamova GV, Lim VI, Teraoka Y, Nierhaus KH (2002) How does tmRNA move through the ribosome? *FEBS Lett* **514:** 55–59

Jossinet F, Ludwig TE, Westhof E (2010) Assemble: an interactive graphical tool to analyze and build RNA architectures at the 2D and 3D levels. *Bioinformatics* **26:** 2057–2059

Jossinet F, Westhof E (2005) Sequence to structure (S2S): display, manipulate and interconnect RNA data from sequence to structure. *Bioinformatics* **21:** 3320–3321

Kaur S, Gillet R, Li W, Gursky R, Frank J (2006) Cryo-EM visualization of transfer messenger RNA with two SmpBs in a stalled ribosome. *Proc Natl Acad Sci USA* **103:** 16484–16489

Keiler KC, Waller PR, Sauer RT (1996a) Role of a peptide tagging system in degradation of proteins synthesized from damaged messenger RNA. *Science* **271:** 990–993

Keiler KC, Waller PRH, Sauer RT (1996b) Role of a peptide tagging system in degradation of proteins synthesized from damaged messenger RNA. *Science* **271:** 990–993

Konno T, Kurita D, Takada K, Muto A, Himeno H (2007) A functional interaction of SmpB with tmRNA for determination of the resuming point of trans-translation. *RNA* **13:** 1723–1731

LeBarron J, Grassucci RA, Shaikh TR, Baxter WT, Sengupta J, Frank J (2008) Exploration of parameters in cryo-EM leading to an improved density map of the E. coli ribosome. *J Struct Biol* **164:** 24–32

Lee S, Ishii M, Tadaki T, Muto A, Himeno H (2001) Determinants on tmRNA for initiating efficient and precise trans-translation: some mutations upstream of the tag-encoding sequence of Escherichia coli tmRNA shift the initiation point of trans-translation *in vitro*. *RNA* **7:** 999–1012

Lei J, Frank J (2005) Automated acquisition of cryo-electron micrographs for single particle reconstruction on an FEI Tecnai electron microscope. *J Struct Biol* **150:** 69–80

Lim VI, Garber MB (2005) Analysis of recognition of transfer-messenger RNA by the ribosomal decoding center. *J Mol Biol* **346:** 395–398

Lin K, Simossis VA, Taylor WR, Heringa J (2005) A simple and fast secondary structure prediction method using hidden neural networks. *Bioinformatics* **21:** 152–159

MacKerell AD, Bashford D, Bellott M, Dunbrack RL, Evanseck JD, Field MJ, Fischer S, Gao J, Guo H, Ha S, Joseph-McCarthy D, Kuchnir L, Kuczera K, Lau FTK, Mattos C, Michnick S, Ngo T, Nguyen DT, Prodhom B, Reiher WE *et al* (1998) All-atom empirical potential for molecular modeling and dynamics studies of proteins. *J Phys Chem B* **102:** 3586–3616

McGuffin LJ, Bryson K, Jones DT (2000) The PSIPRED protein structure prediction server. *Bioinformatics* **16:** 404–405

Metzinger L, Hallier M, Felden B (2008) The highest affinity binding site of small protein B on transfer messenger RNA is outside the tRNA domain. *RNA* **14:** 1761–1772

Miller MR, Healey DW, Robison SG, Dewey JD, Buskirk AR (2008) The role of upstream sequences in selecting the reading frame on tmRNA. *BMC Biol* **6:** 29

Pettersen EF, Goddard TD, Huang CC, Couch GS, Greenblatt DM, Meng EC, Ferrin TE (2004) UCSF Chimera–a visualization system for exploratory research and analysis. *J Comput Chem* **25:** 1605–1612

Phillips JC, Braun R, Wang W, Gumbart J, Tajkhorshid E, Villa E, Chipot C, Skeel RD, Kale L, Schulten K (2005) Scalable molecular dynamics with NAMD. *J Comput Chem* **26:** 1781–1802

Pollastri G, Przybylski D, Rost B, Baldi P (2002) Improving the prediction of protein secondary structure in three and eight classes using recurrent neural networks and profiles. *Proteins* **47:** 228–235

Rath BK, Frank J (2004) Fast automatic particle picking from cryo-electron micrographs using a locally normalized cross-correlation function: a case study. *J Struct Biol* **145:** 84–90

Rudinger-Thirion J, Giege R, Felden B (1999) Aminoacylated tmRNA from Escherichia coli interacts with prokaryotic elongation factor Tu. *RNA* **5:** 989–992

Scheres SH, Gao H, Valle M, Herman GT, Eggermont PP, Frank J, Carazo JM (2007) Disentangling conformational states of macromolecules in 3D-EM through likelihood optimization. *Nat Methods* **4:** 27–29

Schuwirth BS, Borovinskaya MA, Hau CW, Zhang W, Vila-Sanjurjo A, Holton JM, Cate JH (2005) Structures of the bacterial ribosome at 3.5 A resolution. *Science* **310:** 827–834

Shaikh TR, Gao H, Baxter WT, Asturias FJ, Boisset N, Leith A, Frank J (2008) SPIDER image processing for single-particle reconstruction of biological macromolecules from electron micrographs. *Nat Protoc* **3:** 1941–1974

Trabuco LG, Villa E, Mitra K, Frank J, Schulten K (2008) Flexible fitting of atomic structures into electron microscopy maps using molecular dynamics. *Structure* **16:** 673–683

Trimble MJ, Minnicus A, Williams KP (2004) tRNA slippage at the tmRNA resume codon. *RNA* **10:** 805–812

Tu GF, Reid GE, Zhang JG, Moritz RL, Simpson RJ (1995) C-terminal extension of truncated recombinant proteins in Escherichia coli with a 10Sa RNA decapeptide. *J Biol Chem* **270:** 9322–9326

Valle M, Gillet R, Kaur S, Henne A, Ramakrishnan V, Frank J (2003) Visualizing tmRNA entry into a stalled ribosome. *Science* **300:** 127–130

Vila-Sanjurjo A, Ridgeway WK, Seymaner V, Zhang W, Santoso S, Yu K, Cate JH (2003) X-ray crystal structures of the WT and a hyper-accurate ribosome from Escherichia coli. *Proc Natl Acad Sci USA* **100:** 8682–8687

Watts T, Cazier D, Healey D, Buskirk A (2009) SmpB contributes to reading frame selection in the translation of transfer-messenger RNA. *J Mol Biol* **391:** 275–281

Watts T, Healey D, Jones D, Buskirk A (2008) The role of tmRNA nucleotides and the SmpB protein in setting the translational frame on tmRNA. *FASEB J* **22:** 224

Weis F, Bron P, Rolland JP, Thomas D, Felden B, Gillet R (2010) Accommodation of tmRNA-SmpB into stalled ribosomes: a cryo-EM study. *RNA* **16:** 299–306

Williams KP, Martindale KA, Bartel DP (1999) Resuming translation on tmRNA: a unique mode of determining a reading frame. *EMBO J* **18:** 5423–5433

Wower IK, Zwieb C, Wower J (2004) Contributions of pseudoknots and protein SmpB to the structure and function of tmRNA in trans-translation. *J Biol Chem* **279:** 54202–54209

Wower IK, Zwieb C, Wower J (2005) Transfer-messenger RNA unfolds as it transits the ribosome. *RNA* **11:** 668–673